AD-A179 630 SOLAR ACTIVE REGION PHYSICAL PARAMETERS INFERRED FROM A THERMAL CYCLOTRON..(U) TUFTS UNIV MEDFORD MA DEPT OF PHYSICS AND ASTRONOMY K R LANG ET AL. 1986 1/1

UNCLASSIFIED N00014-86-K-0060 F/G 3/2 NL

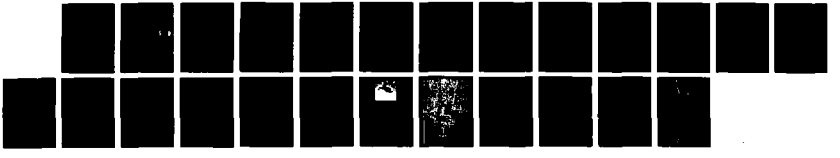

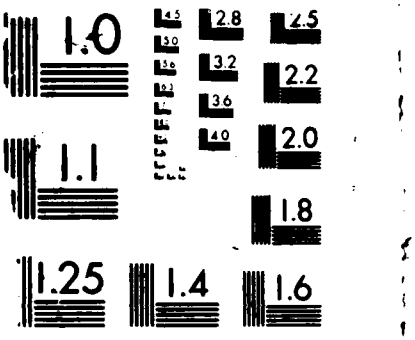

IX. VLA-SMM PAPERS SUBMITTED TO THE ASTROPHYSICAL JOURNAL

K. SOLAR ACTIVE REGION PHYSICAL PARAMETERS INFERRED FROM A THERMAL CYCLOTRON LINE AND SOFT X-RAY SPECTRAL LINES

Kenneth R. Lang and Robert F. Willson
Department of Physics and Astronomy
Tufts University
Medford, Massachusetts

and

Kermit L. Smith and Keith T. Strong
Lockheed Palo Alto Research Laboratory
Palo Alto, California

AFOSR-83-0019
N00014-86-K-0068

ABSTRACT

We present simultaneous high-resolution observations of coronal loops at 20-cm wavelength with the ~~VLA~~ Very Large Array and at soft X-ray wavelengths with the SMM-FCS. The images at 20 cm and soft X-ray wavelengths have nearly identical sizes and ellipsoidal shapes, with a linear extent of about 5×10^9 cm. This emission stretches between and across regions of opposite magnetic polarity in the underlying photosphere. Complete X-ray coronal loops can therefore be imaged at 20 cm, and the VLA maps describe the radio wavelength counterpart of X-ray coronal loops. X-ray spectral lines were used to obtain values of electron temperature $T_e = 2.6 \pm 0.1 \times 10^6$ K and electron density $N_e = 3.1 \pm 0.3 \times 10^9$ cm^{-3}, averaged over the emitting area. These parameters are used with plausible estimates for the loop thickness, magnetic scale height and magnetic field strength to show that the plasma is optically thin to thermal bremsstrahlung and optically thick to thermal gyroresonance radiation at 20 cm. The absence of detectable circular polarization is consistent with an optically thick plasma. The observed brightness temperature was roughly equal to the electron temperature of the coronal plasma. The VLA maps at 10 closely spaced frequencies between 1440 and 1720 MHz describe the same coronal loops or arcades of loops. A plot of the maximum brightness temperature of these loops as a function of observing frequency exhibits a line-like feature with a central frequency of 1650 MHz and a half-width of 80 MHz. This spectral feature is attributed to a thermal cyclotron line and indicates that the optical depth of thermal gyroresonance radiation must be greater than that of thermal bremsstrahlung at these frequencies. The X-ray values for T_e and N_e are combined with plausible values of magnetic scale height and optical depth for gyroresonance absorption to show that the harmonic of the gyrofrequency is 4. The central frequency and narrow width of the thermal cyclotron line are combined with this harmonic to show that the magnetic field strength of the coronal loops is 147 ± 5 G.

INTRODUCTION

Very Large Array (VLA) observations of solar active regions at 20-cm wave-length delineate loop-like features that are probably the radio wavelength counterpart of the coronal loops seen at X-ray wavelengths. The 20-cm coronal loops stretch across regions of opposite magnetic polarity and have sizes, shapes, and temperatures that are similar to those of X-ray coronal loops (Lang, Willson and Rayrole 1982; Lang, Willson and Gaizauskas 1983; Lang and Willson 1983, 1984). Because the radio brightness temperatures are nearly equal to the electron temperatures of coronal loops, the radio radiation is most likely due to a thermal radiation mechanism.

The two possible thermal processes are thermal bremsstrahlung, or free-free emission, and thermal gyroresonance radiation, or cyclotron emission. The electron temperatures and electron densities inferred from X-ray observations of coronal loops can be consistent with either optically thin or optically thick thermal bremsstrahlung at 20-cm wavelength, but these parameters can also be combined with plausible estimates of the coronal magnetic field strength to show that thermal gyroresonance radiation can also become optically thick at this wavelength (McConnell and Kundu 1983; Shevgaonkar and Kundu 1984).

When thermal gyroresonance dominates, one might detect individual cyclotron lines as narrow-band enhancements in the radio spectra of coronal loops. Theoreticians have predicted that such thermal cyclotron lines might be observed if the radiation is emitted from relatively thin layers in the corona where the magnetic field is nearly constant (Syrovatskii and Kuznetsov 1980; Zheleznyakov and Zlotnik 1980; Kuznetsov and Syrovotskii 1981). The spectrum of a line-like feature was subsequently observed at wavelengths near 20 cm when the apex of a coronal loop was resolved (Willson 1985). Observations of these lines provide an unusually accurate method of specifying the coronal magnetic field strength. The

central frequency of the line must be a harmonic of the gyrofrequency, and the narrow linewidth provides tight constraints on that frequency and the relevant magnetic field strength.

Although there have been rapid recent developments in the observations of 20-cm coronal loops, there have been relatively few comparisons of simultaneous 20-cm and soft X-ray observations. Such comparisons can help specify the dominant 20-cm radiation mechanism, while also establishing the physical parameters of the coronal plasma. X-ray spectral lines can, for example, be used to calculate the electron temperature and electron density while the radio observations can uniquely specify the strength and structure of the magnetic field.

In this paper, we provide an example in which the coronal radiation at 20-cm and X-ray wavelengths coincide. The observations are presented in §II, where we also present radio spectra that are attributed to a thermal cyclotron line. In §III, we provide values for the electron density, electron temperature, and magnetic field strength in these coronal loops and attribute the 20-cm radiation to thermal gyroresonance emission. The X-ray values of electron density and electron temperature are combined with the 20-cm brightness temperature and the cyclotron line to calculate the harmonic of the gyrofrequency. Our results are summarized in §IV.

II. OBSERVATIONS

We have used the VLA and the SMM-FCS to observe the solar active region AR 4663 on 1985 June 7. The VLA was used in the B configuration at 10 different wavelengths between 21.8 cm (1440 MHz) and 17.4 cm (1720 MHz) with bandwidths of 12.5 MHz between 1500 UT and 2400 UT on June 7, and the FCS observed five prominent soft X-ray lines (O VIII, Mg XI, Si XIII, S XV and Fe XXV) between 1500 UT and 1940 UT on June 7. The position of AR 4663 on the solar surface was 01° N and 65° E at 1300 UT on June 7.

The half-power beamwidth of the individual VLA antennae ranged between 26' and 31', and the synthesized maps constructed from up to 325 interferometer pairs had beamwidths between 3.0" x 3.5" and 3.6" x 4.2". The active region was observed with the VLA at successive pairs of wavelengths for 5 min. each, so that all 10 wavelengths could be observed in 25 min.. This sequence of observations was followed by successive 2 min. observations of the calibrator source PKS 0552 + 398 whose flux density was 1.7 Jy at 1465 MHz. The calibrated data for the 9 hour interval were used with the standard CLEAN procedure to make synthesis maps of both the total intensity, I, and circular polarization or Stokes parameter V. No solar bursts or flares were observed during this interval, and the synthesis maps therefore refer to the quiescent, or non-flaring, radio emission. There was no detectable circular polarization ($V/I < 15\%$) suggesting that the region was optically thick to both the extraordinary and ordinary modes of wave propagation at 20-cm wavelength.

The 14" collimated field of view of the FCS was rastered over a 4' x 4' area with a pixel spacing of 10" x 10". X-ray images were obtained simultaneously in the five soft X-ray emission lines every 990 s throughout the orbital day which lasts about 60 min. All of the available data for each spectral line during each orbit were then summed and averaged to improve the statistical uncertainty on the

count rate from each pixel. Significant emission was detected in the two softest channels -O VIII and Mg XI. The peak formation temperatures for these lines are 3 x 10^6 K and 7 x 10^6 K, respectively. The failure to detect emission in the harder, more energetic channels indicates that the active region was unperturbed by any flaring throughout the period of observation. The SMM Bent Crystal Spectrometer (BCS) confirmed the absence of flares as no significant brightenings were observed in its Ca XIX channel during these observations.

The PCS also produced a white-light image that showed the sunspots, making it possible to align the X-ray images with the sunspots to an accuracy of 10". The VLA maps of the total intensity, I, at 20-cm wavelength were aligned with Hα photographs of the same sunspots with a similar 10" accuracy. This enabled us to compare the soft X-ray and 20 cm data for the same field of view and angular scale.

The 20.3-cm (1480 MHz) radiation and the soft X-ray (O VIII) emission originated in the same area (Figure 1). Observations at both wavelengths apparently describe the same coronal loops or arcades of loops. They are about 60" across, which corresponds to a linear extent, L, of about 5 x 10^9 cm. Both the radio and the X-ray emission stretch between and across regions of opposite magnetic polarity seen in magnetograms of the underlying photosphere (Figure 2).

The radio-wavelength coronal loops exhibited the same ellipsoidal shape and extent at 10 closely spaced frequencies ranging from between 1440 MHz (20.8 cm) and 1725 MHz (17.4 cm) (Figure 3). The maximum brightness temperatures are given in Table 1 and plotted as a function of observing frequency in Figure 4. This spectrum contains a line-like feature with a central frequency, ν, 1650 MHz and a full-width-to-half-maximum, $\Delta\nu$, of 80 MHz. As discussed in more detail in §III, we

attribute this feature to a thermal cyclotron line and use it to obtain an accurate estimate of the coronal magnetic field strength.

III. DISCUSSION

To identify the dominant thermal radiation mechanism at 20 cm, one needs to know the electron temperature, electron density, and the magnetic field strength. The X-ray data were therefore used to infer the mean electron temperature, T_e, and the mean electron density, N_e, for the regions marked A, B, and C in Figure 5. As previously mentioned, the active region was so quiescent and was only detectable in the two softest X-ray channels (O VIII and Mg XI). The ratios of the two lines (O VIII to Mg XI) were used as temperature diagnostics.

An emission measure was inferred from the temperature and the observed X-ray fluxes. The electron density was then calculated using a volume of 3×10^{27} cm^3, which equals the product of the FCS pixel area and a typical soft X-ray scale height of 3×10^9 cm.

The mean temperatures and densities are given in Table 2. We obtain average values of $T_e = 2.6 \pm 0.1 \times 10^6$ K and $N_e = 3.1 \pm 0.3 \times 10^9$ cm^{-3} when averaged over all the coronal loops or arcades of loops. Here, the uncertainties correspond to the maximum possible deviation that reproduces the flux in all the detected X-ray lines to within 1 standard deviation of the observed values. The inferred values of electron temperature and electron density are typical of those of quiescent coronal active region loops. Within the uncertainties, the observed loops were isothermal and isobaric, but there was a statistically uncertain tendency for a hotter temperature at the loop apex.

We may use the parameters derived from X-ray observations to estimate the optical depth and brightness temperature of the X-ray emitting plasma at radio wavelengths. Assuming an isothermal source of electron temperature, T_e, and optical depth, τ, the observed radio brightness temperature, T_B, will be given by

$$T_B = \tau\, T_e \qquad \text{for } \tau \ll 1 \text{ (optically thin)}$$

and (1)

$$T_B = [\, 1 - \exp(-\tau)\,]\, T_e \qquad \text{for } \tau \gg 1 \text{ (optically thick).}$$

The free-free optical depth, τ_{f-f}, for an isothermal loop with electron temperature, T_e, and width or thickness, W, is (Lang 1980)

$$\tau_{f-f} = 9.8 \times 10^{-3} \frac{N_e^2 W}{\nu^2\, T_e^{3/2}} \ln\left(4.7 \times 10^{10} \frac{T_e}{\nu}\right) , \qquad (2)$$

where ν is the observing frequency in Hz and N_e is the electron density in cm^{-3}. Using $\nu = 1.65 \times 10^9$ Hz, corresponding to the center of our line-like feature, together with the X-ray values of $T_e = 2.6 \times 10^6$ K and $N_e = 3.1 \times 10^9$ cm^{-3} and a typical loop thickness of $W \leq 1 \times 10^9$ cm in equation (2), we obtain $\tau_{f-f} \leq 0.14$. The plasma is therefore optically thin to thermal bremsstrahlung at this frequency, and the bremsstrahlung brightness $T_B \leq 3.6 \times 10^5$ K is an order of magnitude lower than the observed brightness temperature.

We must therefore examine the alternative possibility of thermal gyroresonance radiation. The optical depth, τ_{g-r}, due to gyroresonance absorption is given by (Zheleznyakov 1970):

$$\tau_{g-r} = 2\pi^2 \frac{n^{2n}}{2^{n+1} n!} \frac{\nu_p^2}{c\nu} \left(\frac{kT_e}{mc^2}\right)^{n-1} L_H \, (1 \pm \cos\alpha)^2 \sin^{2n-2}\alpha \qquad (3)$$

where $n = 1, 2, 3, \ldots$ is the harmonic number, the plasma frequency $\nu_p = 8.9 \times 10^3 N_e^{1/2}$ Hz, the velocity of light $c = 2.9979 \times 10^{10}$ cm s^{-1}, Boltzmann's constant $k = 1.38 \times 10^{-16}$ erg K^{-1}, the electron mass $m = 9.1 \times 10^{-28}$ g, the scale height of the magnetic field is L_H, and α is the angle between the line of sight and the direction of the magnetic field lines. Collecting terms, we obtain

$$\tau_{g-r} = 0.052 \frac{n^{2n}}{2^{n+1} n!} \frac{N_e}{\nu} (1.7 \times 10^{-10} T_e)^{n-1} L_H \, (1 \pm \cos\alpha)^2 \sin^{2n-2}\alpha \qquad (4)$$

The harmonic n is related to the observing frequency ν and the magnetic field strength H through the relation

$$\nu = 2.8 \times 10^6 \, nH \quad \text{Hz} \qquad (5)$$

For gyroresonance absorption to dominate free-free absorption at our reference frequency $\nu = 1.65 \times 10^9$ Hz, the layers must be optically thick with

$\tau_{g-r} > \tau_{f-f} \approx 0.14$. We will adopt $\tau_{g-r} \approx 1.0$ and determine the harmonic number, n. If we assume a magnetic scale height $L_H = 1 \times 10^9$ cm and $\alpha = 65°$, the solar longitude of AR 4663, then we may use these parameters together with the X-ray values of $N_e = 3.1 \times 10^9$ cm^{-3} and $T_e = 2.6 \times 10^6$ K in equation (4) to obtain n = 4.

To put it another way, the fourth harmonic of the gyrofrequency becomes optically thick to gyroresonance absorption with $T_B \approx T_e$ and $\tau_{g-r} > \tau_{f-f}$. We can use equation (6) with n = 4 and $\nu = 1.65 \times 10^9$ Hz to obtain a magnetic field strength of H = 147 G. This is consistent with model calculations of the spectrum of another thermal cyclotron line in which n = 4 or possibly n = 5, with H = 145 G or possibly H = 119 G (Willson 1985), but in the case presented here, we do not have to make ad hoc assumptions about N_e and T_e. Observations of these lines provide an unusually accurate method of specifying the coronal magnetic field strength. For instance, the observed line half width is only 80 mHz, indicating that H is known with a precision of better than 5 G or H = 147 ± 5 G.

However these are general arguments based upon homogeneous, isothermal models. When Table 1 and Figure 4 are examined in greater detail, we notice that inhomogeneities are required. For example, the 20-cm brightness temperture, T_B, is usually lower than the electron temperature, T_e, suggesting that the radio emission from the hot, optically thick loops is partially absorbed in a cooler external plasma. In addition, the T_B at 1650 MHz is greater than T_e, suggesting a thin, hot gyroresonance layer similar to that proposed by Willson (1985). The detailed radio spectrum is probably due to a mixture of hot and cool loops whose average properties are inferred from X-ray observations.

Here, we should point out that individual cyclotron lines are observed near the apex of coronal loops where the magnetic field is relatively constant and a steep temperature gradient may exist. Neutral currents might also play a role, leading to intense radio emission from a relatively thin layer near the loop apex. The cyclotron lines from loop legs will, however, exhibit a great deal of spatial structure if the loops are thin enough (Holman and Kundu 1985). Observations of thin loops at an oblique angle with wavelengths of about 6 cm should lead to the spatial resolution of cyclotron-emitting layers along the loop legs, while observations of the loop apex at λ = 20 cm can resolve cyclotron lines in this region. Both techniques can provide a powerful diagnostic of the magnetic and thermal properties of coronal loops.

IV. SUMMARY

Simultaneous high-resolution observations of AR 4663 with the VLA and the SMM-FCS indicate that the radiation at 20-cm and soft X-ray wavelengths originates from the same region, and that 20-cm VLA maps can image X-ray coronal loops. The X-ray spectral lines were used to infer an average electron temperature of about $2.9 \pm 0.1 \times 10^6$ K and an average electron density of $3.1 \pm 0.3 \times 10^9$ cm^{-3}. These parameters were used to show that the layers emitting 20-cm radiation can be optically thick to either thermal bremsstrahlung or thermal gyroresonance radiation, depending upon unknown but plausible values of loop thickness, magnetic scale height and magnetic field strength.

The absence of circular polarization suggests that these coronal loops are optically thick at wavelengths near 20 cm and the detection of a line-like feature in the radio spectrum indicates that gyroresonance absorption exceeds free-free absorption. This feature is attributed to a thermal cyclotron line. The X-ray values for T_e and N_e were combined with plausible values for gyroresonant optical depth and the magnetic scale height to show that the 20-cm radiation is probably at the fourth harmonic of the gyrofrequency. The central frequency and relatively narrow width of the thermal cyclotron line were combined with this harmonic to infer a magnetic field strength of 147 ± 5 G at the apexes of these coronal loops.

Radio astronomical studies of the Sun at Tufts University are supported under grant AFOSR-83-0019 with the Air Force Office of Scientific Research and contract N00014-86-K-0068 with the Office of Naval Research (ONR). Simultaneous VLA and SMM observations of the Sun are supported by NASA grant NAG 5-501. K.L.S. and K.T.S. are supported by NASA contract NAS 5-23758 and the Lockheed Independent Research Program. The FCS and BCS were built by a consortium of three groups: Lockheed Palo Alto Research Laboratory, Mullard Space Science Laboratory, and the Rutherford Appleton Laboratories. The VLA is operated by Associated Universities Inc., under contract with the National Science Foundation.

REFERENCES

Holman, G.O., and Kundu, M.R. 1985, Ap. J. 292, 291.

Kuznetsov, V.S., and Syrovatskii, S.I. 1981, Solar Phys. 69, 391.

Lang, K.R. 1980, Astrophysical Formulae (2nd ed., New York: Springer Verlag), p.47.

Lang, K.R., and Willson, R.F. 1983, Adv. Space Res. 2, No. 11, 91.

Lang, K.R., and Willson, R.F. 1984, Adv. Space Res. 4, No. 7, 105.

Lang, K.R., and Willson, R.F. and Gaizauskas, V. 1983, Ap. J. 267, 455.

Lang, K.R., Willson, R.F., and Rayrole, J. 1982, Ap. J. 258, 384.

McConnell, D., and Kundu, M.R. 1983, Ap. J. 269, 698.

Shevgaonkar, R.K., and Kundu, M.R. 1984, Ap. J. 283, 413.

Syrovatskii, S.I., and Kuznetsov, V.D. 1980, in IAU Symposium 86, Radio Physics of the Sun, ed. M.R. Kundu and T.E. Gergely (Dordrecht: Reidel), p. 109.

Willson, R.F. 1985, Ap. J. 298, 911.

Zheleznyakov, V.V. 1970, Radio Emission of the Sun and Planets (New York: Pergamon Press), p. 454.

Zheleznyakov, V.V., and Zlotnik, E. Ya. 1980, in IAU Symposium 86 Radio Physics of the Sun, ed. M.R. Kundu and T. Gergely (Dordrecht: Reidel). p. 87.

KENNETH R. LANG and ROBERT F. WILLSON
Department of Physics and Astronomy,
Robinson Hall,
Tufts University,
Medford, MA 02155

KERMIT L. SMITH and KEITH T. STRONG
Code 602.6,
Bldg. 7 - XRP,
Goddard Space Flight Center,
Greenbelt, MD 20771

Table 1. Maximum brightness temperatures, T_{Bmax}, of the coronal loops within AR 4336 at different radio frequencies.

Frequency (MHz)	T_{Bmax} (10^6 K)	Frequency (MHz)	T_{Bmax} (10^6 K)
1440	1.7	1620	2.8
1480	1.9	1658	3.8
1515	2.0	1690	2.4
1558	2.3	1705	2.0
1585	2.2	1725	1.8

Table 2. The mean electron temperature, T_e, and the mean electron density, N_e, for the regions marked A, B, and C in Figure 5. Values averaged over all three regions are given at the bottom of each column.

Region	Te (10^6 K)	N_e (10^9 cm^{-3})
A	2.8	2.1
B	2.7	3.2
C	2.2	3.6
Average	2.6	3.1

FIGURE LEGENDS

Fig. 1. A comparison of 20 cm (VLA-left), soft X-ray (SMM-FCS-center) and Hα (SOON-right) images of AR 4663 on 1985 June 7. The field of view of all three images is identical, and the identical angular scale can be inferred from the 60" spacing between fiducial marks on the axes. The contours of the 20 cm map mark levels of equal brightness temperature corresponding to 0.2, 0.4,...1.0 times the maximum brightness temperature of 1.8×10^6 K. The soft X-ray data were taken in the O VIII line (18.9 Å) with contours corresponding to 3, 7, 14 and 24 counts s^{-1} above a background level of 10 counts s^{-1} with a maximum signal of 18 counts s^{-1}.

Fig. 2. The 20 cm contours of equal brightness temperature (solid black lines) are superposed on a Kitt Peak National Observatory (KPNO) magnetogram of AR 4663 on 1985 June 7. The black magnetogram features indicate regions of negative magnetic polarity with magnetic fields pointed in toward the Sun, while the white magnetogram areas are regions of positive magnetic polarity with magnetic field lines pointed out toward the observer. The KPNO magnetogram is coutesy of Jack Harvey of the National Solar Observatory.

Fig. 3. VLA synthesis maps of the total intensity, I, of AR 4663 at 10 closely spaced frequencies during a 9 hour period on 1985 June 7. The synthesized beamwidth was about 3" x 4", and the spacing between fiducial marks on the axes is 60". The map contours mark levels of equal brightness temperature, with an outermost contour of 7.6×10^5 K and a contour interval of 3.8×10^5 K. The maximum brightness temperatures are given in Table 1 and plotted in Figure 4.

Fig. 4. The maximum brightness temperature of the coronal loops of AR 4663 at 10 closely spaced frequencies on 1985 June 7. The maximum temperatures were inferred from the 9-hour synthesis maps shown in Figure 3, and the error bars correspond to the peak-to-peak fluctuations in the background temperature of the synthesis maps.

Fig. 5. A soft X-ray map of AR 4663 taken in the O VIII line (18.9 Å) with contours corresponding to 3, 7 and 14 counts s^{-1}. The image represents the sum of two maps taken at 15:11 UT and 19:55 UT on 1985 June 7. Each map took 590 s to accumulate. The ratio of the O VIII and Mg XI line intensities were used to determine the mean electron temperature in the regions marked A, B, and C. These temperatures are given together with estimates for the mean electron density in Table 2.

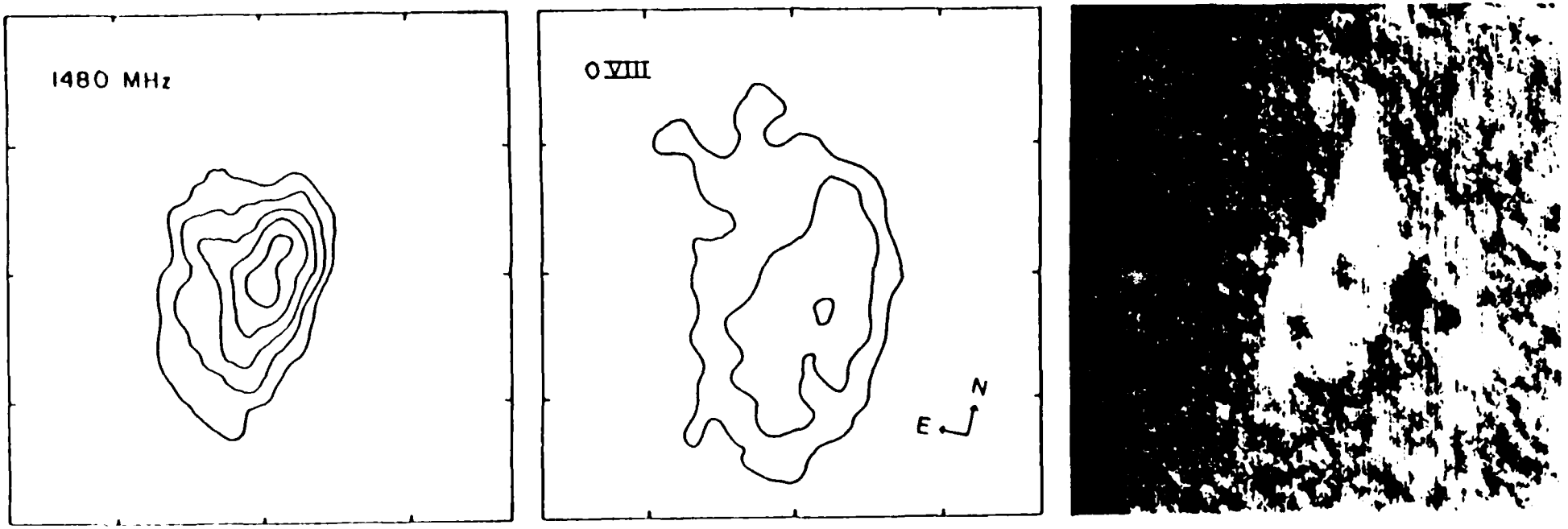

Figure 1.

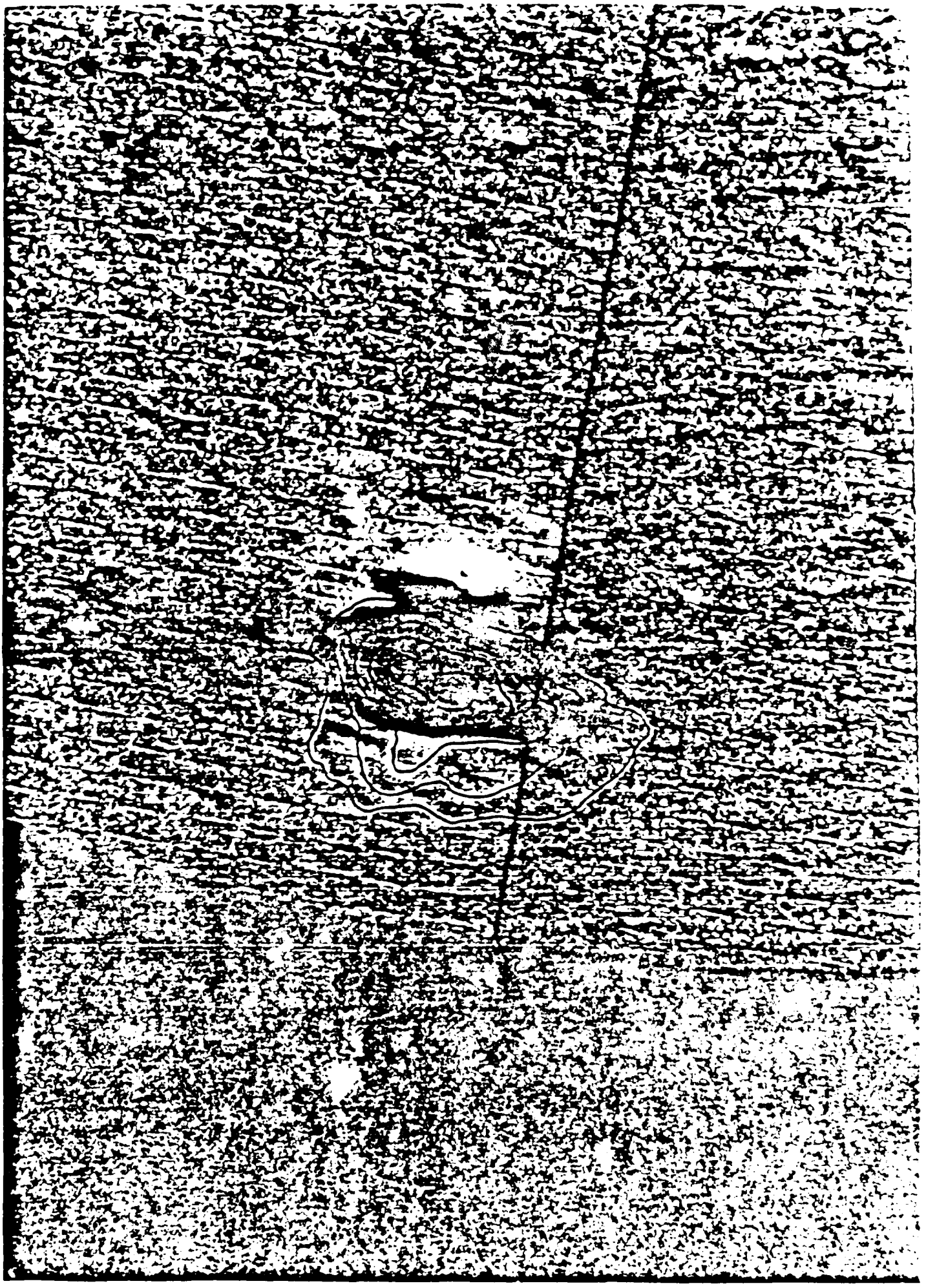

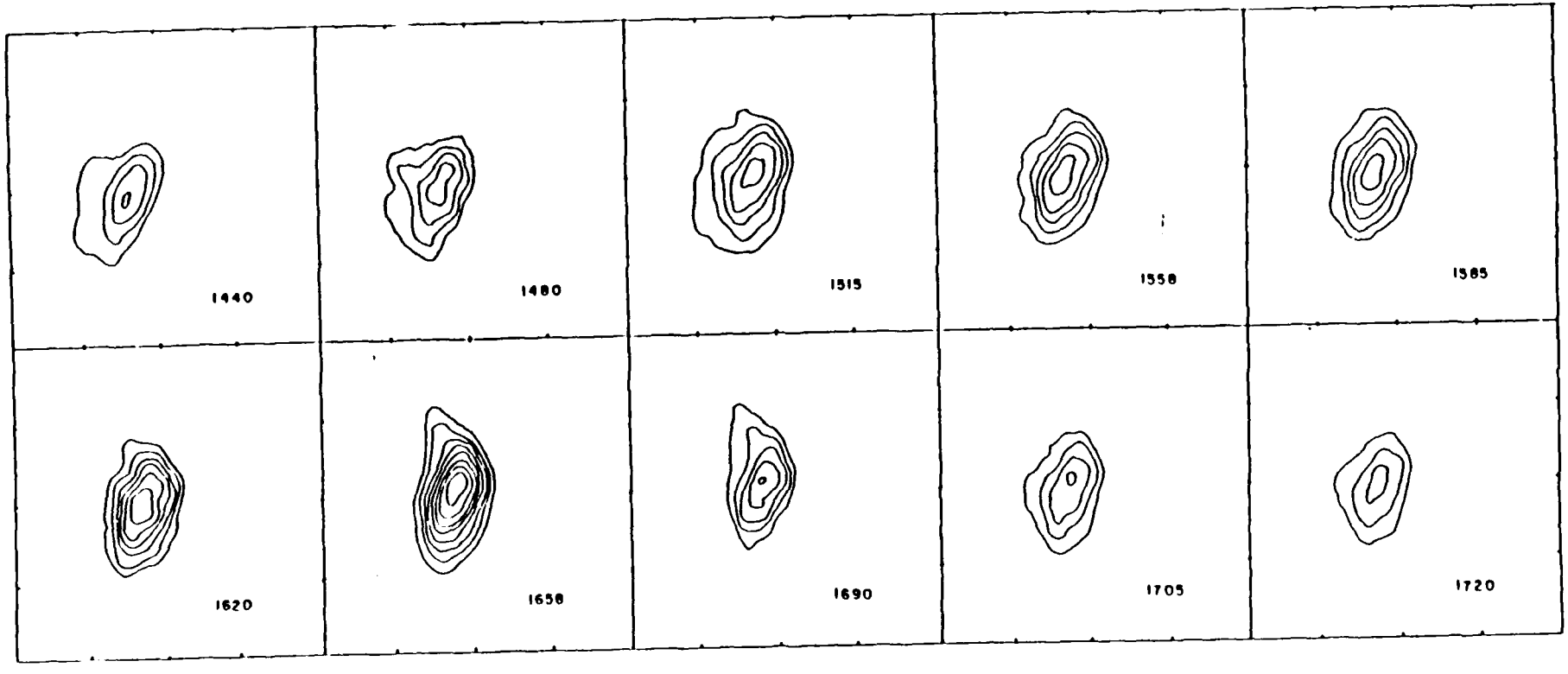

Figure 3.

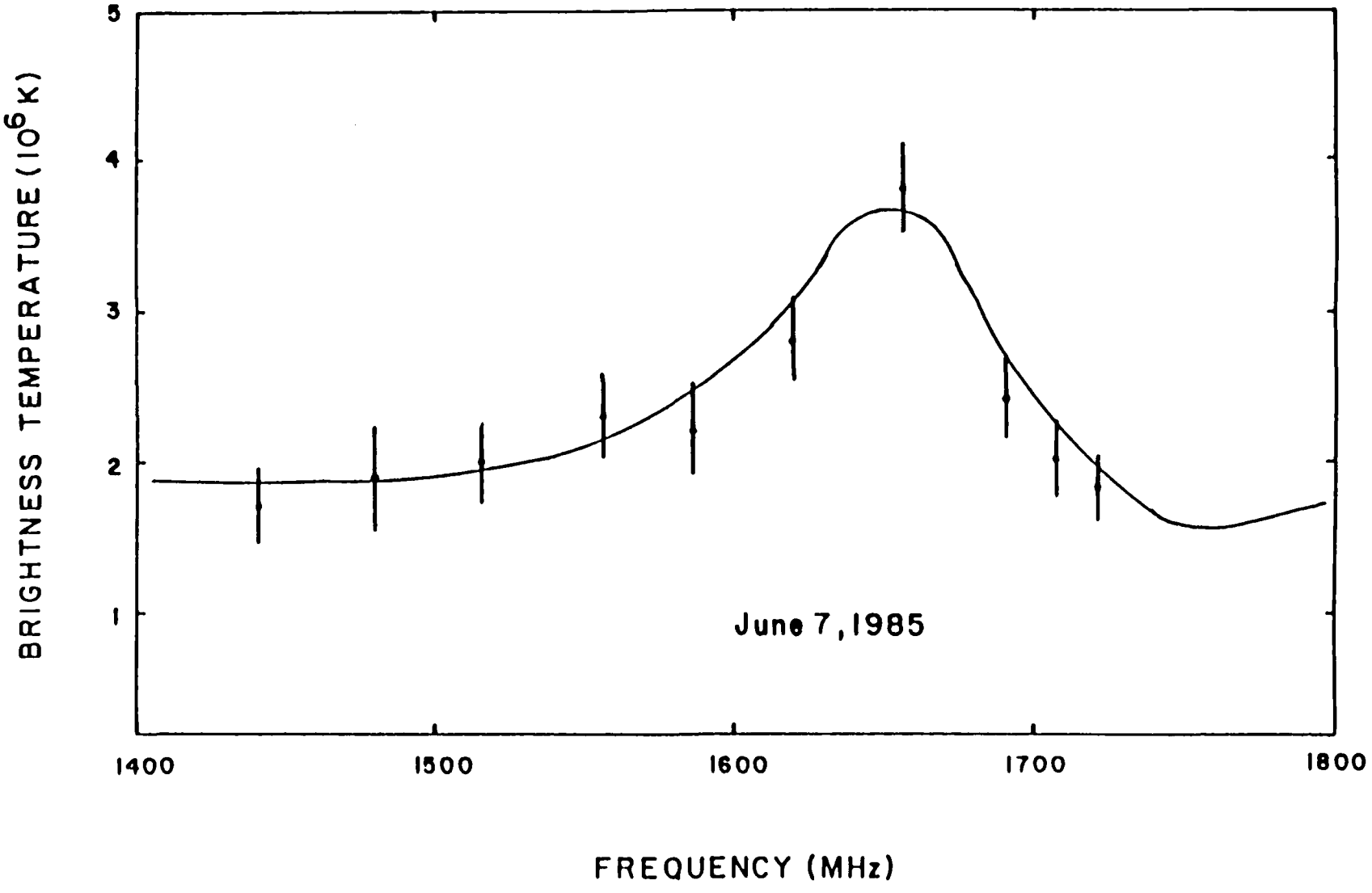
BRIGHTNESS TEMPERATURE (10^6 K)
5
4
3
2
1
June 7, 1985
1400
1500
1600
1700
1800
FREQUENCY (MHz)

Figure 4.

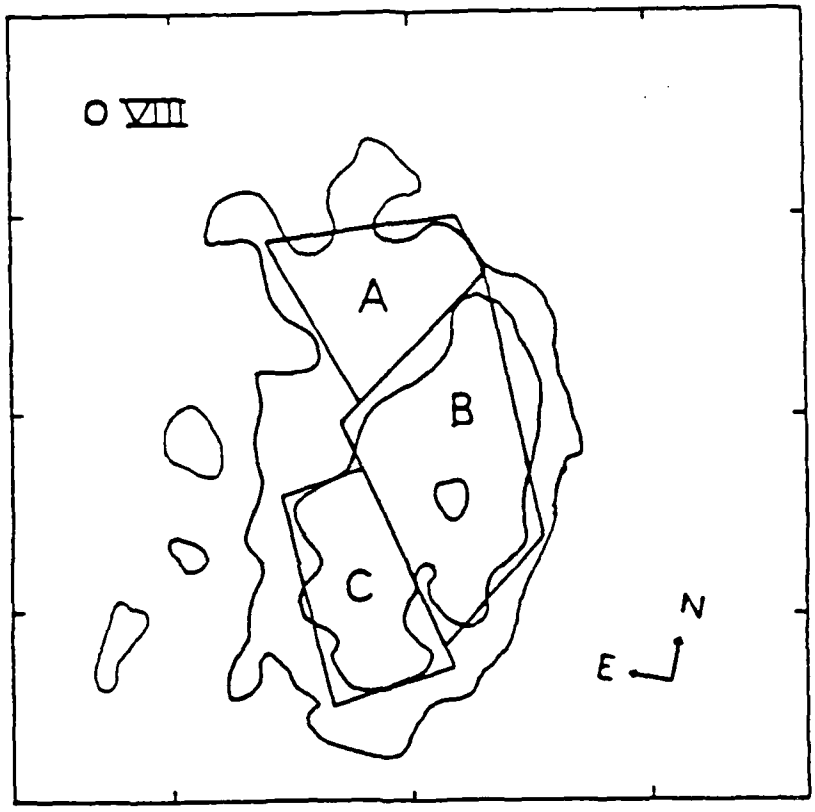

Figure 5.

END

5-87

DTIC